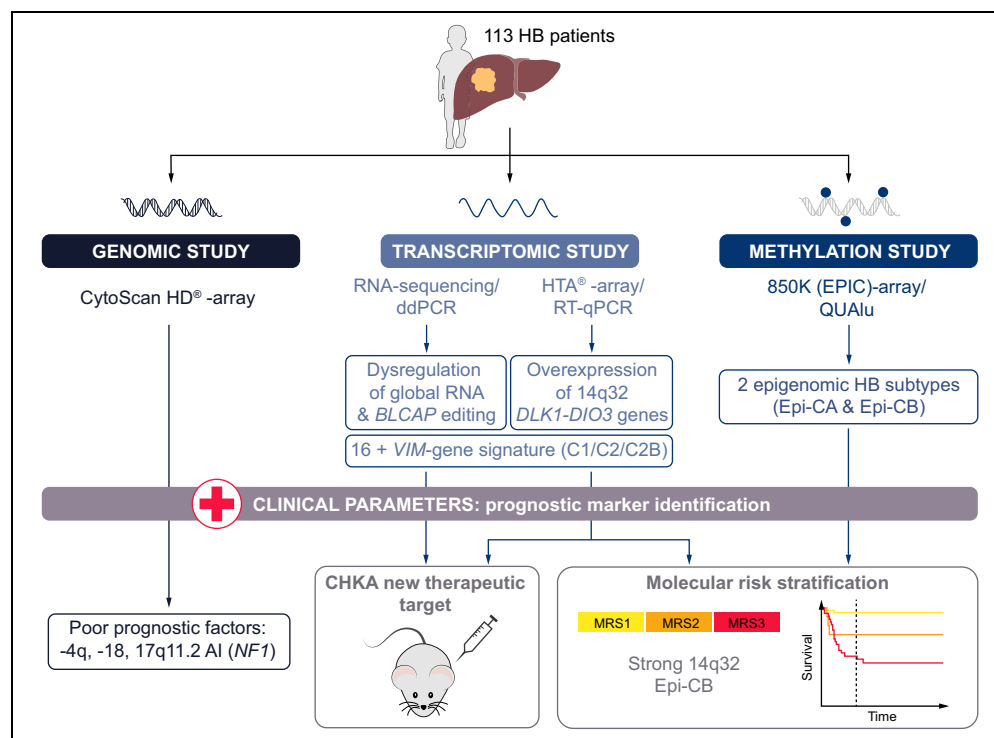


Epigenetic footprint enables molecular risk stratification of hepatoblastoma with clinical implications

Graphical abstract



Authors

Juan Carrillo-Reixach,
Laura Torrens,
Marina Simon-Coma, ...,
Maria Rosa Sarrias, Josep
M. Llovet,
Carolina Armengol

Correspondence

carmengol@igtp.cat
(C. Armengol).

Lay summary

Hepatoblastoma is a rare childhood liver cancer that has been understudied. We have used cutting-edge technologies to expand our molecular knowledge of this cancer. Our biological findings can be used to improve clinical management and pave the way for the development of novel therapies for this cancer.

Highlights

- Hepatoblastoma (HB) involves global dysregulation of RNA editing, including in the tumor suppressor *BLCAP*.
- Overexpression of a 300 kb region within the 14q32 *DLK1/DIO3* locus is a new hallmark of HB.
- We identified 2 epigenomic HB subtypes -Epi-CA and Epi-CB- with distinct degrees of DNA hypomethylation and CpG island hypermethylation.
- The molecular risk stratification of HB, based on the 14q32-signature and epigenomic subtypes, is associated with patient outcomes.
- The enzyme CHKA could be a novel therapeutic target for patients with HB.

<https://doi.org/10.1016/j.jhep.2020.03.025>

© 2020 European Association for the Study of the Liver. Published by Elsevier B.V. This is an open access article under the CC BY-NC-ND license (<http://creativecommons.org/licenses/by-nc-nd/4.0/>). J. Hepatol. 2020, 73, 328–341



Epigenetic footprint enables molecular risk stratification of hepatoblastoma with clinical implications

Juan Carrillo-Reixach¹, Laura Torrens^{2,3}, Marina Simon-Coma^{1,4}, Laura Royo¹,
Montserrat Domingo-Sàbat¹, Jordi Abril-Fornaguera^{2,3}, Nicholas Akers^{3,5}, Margarita Sala^{4,6,7},
Sonia Ragull¹, Magdalena Arnal⁸, Núria Villalmanzo⁹, Stefano Cairo^{10,11}, Alberto Villanueva¹²,
Roland Kappler¹³, Marta Garrido¹⁴, Laura Guerra¹⁵, Constantino Sábado¹⁶, Gabriela Guillén¹⁷,
Mar Mallo¹⁸, David Piñeyro¹⁹, María Vázquez-Vitali¹, Olga Kuchuk², María Elena Mateos²⁰,
Gema Ramírez²¹, Manuel López Santamaría²², Yasmina Mozo²³, Aroa Soriano²⁴,
Michael Grotzer²⁵, Sophie Branchereau²⁶, Nagore García de Andoin²⁷, Blanca López-Ibor²⁸,
Ricardo López-Almaraz²⁹, José Antonio Salinas³⁰, Bárbara Torres³¹, Francisco Hernández²²,
José Javier Uriz²⁷, Monique Fabre³², Julià Blanco^{33,34}, Claudia Paris³⁵, Viera Bajčiová³⁶,
Geneviève Laureys³⁷, Helena Masnou⁶, Ariadna Clos⁶, Cristina Belendez³⁸,
Catherine Guettier²⁶, Lauro Sumoy¹⁹, Ramón Planas^{4,6}, Mireia Jordà^{9,39}, Lara Nonell⁸,
Piotr Czauderna⁴⁰, Bruce Morland⁴¹, Daniela Sia², Bojan Losic^{5,42,43,44}, Marie Annick Buendia⁴⁵,
Maria Rosa Sarrias^{4,46}, Josep M. Llovet^{2,3,47}, Carolina Armengol^{1,4,*}

¹Childhood Liver Oncology Group, Germans Trias i Pujol Research Institute (IGTP), Program for Predictive and Personalized Medicine of Cancer (PMPPC), Badalona, Spain; ²Mount Sinai Liver Cancer Program, Divisions of Liver Diseases, Tisch Cancer Institute, Icahn School of Medicine at Mount Sinai, New York, USA; ³Translational research in Hepatic Oncology, Liver Unit, Institut d'Investigacions Biomèdiques August Pi i Sunyer (IDIBAPS), Hospital Clínic, Universitat de Barcelona, Barcelona, Spain; ⁴CIBER, Hepatic and Digestive Diseases, Barcelona, Spain; ⁵Department of Genetics and Genomic Sciences, The Icahn Institute for Genomics and Multiscale Biology, Icahn School of Medicine at Mount Sinai, New York, USA; ⁶Gastroenterology Department, Hospital Universitari Germans Trias i Pujol Hospital, Badalona, Spain; ⁷Gastroenterology Department, Hospital Universitari Josep Trueta, Girona, Spain; ⁸MARGENomics, IMIM (Hospital del Mar Medical Research Institute), Barcelona, Spain; ⁹PMPPC, IGTP, Badalona, Spain; ¹⁰XenTech, Evry, France; ¹¹Instituto di Ricerca Pediatrica, Corso Stati Uniti 4, Padova, Italy; ¹²Chemoresistance and Predictive Factors Group, Program Against Cancer Therapeutic Resistance, Catalan Institute of Oncology (ICO), Bellvitge Biomedical Research Institute, L'Hospitalet del Llobregat, Barcelona, Spain; ¹³Department of Pediatric Surgery, Dr. von Hauner Children's Hospital, Ludwig-Maximilians-University Munich, Lindwurmstr. 2a, 80337 Munich, Germany; ¹⁴Hospital Vall d'Hebron, Pathology Department, Barcelona, Spain; ¹⁵University Hospital La Paz, Pathology Department, Madrid, Spain; ¹⁶Hospital Vall d'Hebron, Pediatric Oncology Department, Barcelona, Spain; ¹⁷Hospital Vall d'Hebron, Pediatric Surgery Department, Barcelona, Spain; ¹⁸MDS Research Group, Josep Carreras Leukaemia Research Institute, ICO-Hospital Germans Trias i Pujol, Universitat Autònoma de Barcelona, Badalona, Spain; ¹⁹High Content Genomics and Bioinformatics Unit, PMPPC, IGTP, Badalona, Spain; ²⁰Pediatric Oncology Unit, Department of Pediatrics, University Hospital Reina Sofía, Córdoba, Spain; ²¹University Hospital Universitario Virgen del Rocío, Pediatric Oncology Department, Sevilla, Spain; ²²University Hospital La Paz, Pediatric Surgery Department, Madrid, Spain; ²³University Hospital La Paz, Pediatric Oncology Department, Madrid, Spain; ²⁴Biomedical Research in Cancer Stem Cells Group, Pathology Department, Institut de Recerca Hospital Vall d'Hebron (VHIR), Barcelona, Spain; ²⁵Department of Pediatric Oncology, University Children's Hospital Zurich, University of Zurich, Zurich, Switzerland; ²⁶Bicêtre Hospital, Le Kremlin-Bicêtre, France; ²⁷Pediatric Oncology, Hospital Universitario Donostia, Doctor Begiristain Kalea, 117, 20080, Donostia, Spain; ²⁸Department of Pediatric Hematology and Oncology, HM Montepíncipe Hospital, Boadilla del Monte, Madrid, Spain; ²⁹Pediatric Oncology and Hematology, Hospital Universitario Cruces, Bilbao, Spain; ³⁰Division of Hematology-Oncology, Department of Pediatrics, Hospital Universitari Son Espases, Palma de Mallorca, Spain; ³¹Medical Oncology Department, Pediatric Oncology Department, University Hospital La Fe, Valencia, Spain; ³²Department of Pathology, Hôpital Universitaire Necker-Enfants Malades, Assistance Publique-Hôpitaux de Paris, and Université Paris Descartes, Paris, France; ³³IrsiCaixa AIDS Research Institute, IGTP, Badalona, Catalonia, Spain; ³⁴University of Vic - Central University of Catalonia, Vic, Spain; ³⁵Stem Cell Transplant Unit, Hospital Luis Calvo Mackenna, Santiago, Chile; ³⁶Department of Pediatric Oncology, Childrens University Hospital Brno, Brno, Czech; ³⁷Department of Pediatric Hematology, Oncology and Hematopoietic Stem Cell Transplantation, Ghent University Hospital, Ghent, Belgium; ³⁸Oncohematology Service, Hospital Gregorio Marañón, Madrid, Spain; ³⁹Consortium for the Study of Thyroid Cancer, CECaT, Barcelona, Spain; ⁴⁰Department of Surgery and Urology for Children and Adolescents, Medical University of Gdansk, Gdansk, Poland; ⁴¹Department of Oncology, Birmingham Women's and Children's Hospital, Birmingham, UK; ⁴²Graduate School of Biomedical Sciences, One Gustave L. Levy Place, Box 1022, New York, NY; ⁴³Tisch Cancer Institute, Cancer Immunology Program, Icahn School of Medicine at Mount Sinai, New York, NY; ⁴⁴Icahn Institute for Data Science and Genomic

Keywords: Hepatoblastoma (HB); RNA editing; *BLCAP*; *14q32*; *DLK1-DIO3* locus; Molecular risk stratification; Prognostic biomarker; *CHKA*.

Received 5 September 2019; received in revised form 11 March 2020; accepted 13 March 2020; available online 30 March 2020

*Corresponding author. Address: Germans Trias i Pujol Research Institute (IGTP), Edifici Muntanya, Campus Can Ruti, Childhood Liver Oncology Group (c-LOG), Ctra.

de Can Ruti. Camí de les Escoles, s/n 08916 Badalona, Spain. Tel.: + 34 93 554 30 72, fax: +34 93 497 86 54.

E-mail address: carmengol@igtp.cat (C. Armengol).

<https://doi.org/10.1016/j.jhep.2020.03.025>



Technology, Icahn School of Medicine at Mount Sinai, New York, NY; ⁴⁵INSERM, UMR 1193, Paul-Brousse Hospital, Hepatobiliary Centre, Villejuif, France; ⁴⁶Innate Immunity Group, IGTP, Badalona, Spain; ⁴⁷Institució Catalana de Recerca i Estudis Avançats (ICREA), Barcelona, Spain

Background & Aims: Hepatoblastoma (HB) is a rare disease. Nevertheless, it is the predominant pediatric liver cancer, with limited therapeutic options for patients with aggressive tumors. Herein, we aimed to uncover the mechanisms of HB pathobiology and to identify new biomarkers and therapeutic targets in a move towards precision medicine for patients with advanced HB.

Methods: We performed a comprehensive genomic, transcriptomic and epigenomic characterization of 159 clinically annotated samples from 113 patients with HB, using high-throughput technologies.

Results: We discovered a widespread epigenetic footprint of HB that includes hyperediting of the tumor suppressor *BLCAP* concomitant with a genome-wide dysregulation of RNA editing and the overexpression of mainly non-coding genes of the oncogenic 14q32 *DLK1-DIO3* locus. By unsupervised analysis, we identified 2 epigenomic clusters (Epi-CA, Epi-CB) with distinct degrees of DNA hypomethylation and CpG island hypermethylation that are associated with the C1/C2/C2B transcriptomic subtypes. Based on these findings, we defined the first molecular risk stratification of HB (MRS-HB), which encompasses 3 main prognostic categories and improves the current clinical risk stratification approach. The MRS-3 category (28%), defined by strong 14q32 locus expression and Epi-CB methylation features, was characterized by *CTNNB1* and *NFE2L2* mutations, a progenitor-like phenotype and clinical aggressiveness. Finally, we identified choline kinase alpha as a promising therapeutic target for intermediate and high-risk HBs, as its inhibition in HB cell lines and patient-derived xenografts strongly abrogated tumor growth.

Conclusions: These findings provide a detailed insight into the molecular features of HB and could be used to improve current clinical stratification approaches and to develop treatments for patients with HB.

Lay summary: Hepatoblastoma is a rare childhood liver cancer that has been understudied. We have used cutting-edge technologies to expand our molecular knowledge of this cancer. Our biological findings can be used to improve clinical management and pave the way for the development of novel therapies for this cancer.

© 2020 European Association for the Study of the Liver. Published by Elsevier B.V. This is an open access article under the CC BY-NC-ND license (<http://creativecommons.org/licenses/by-nc-nd/4.0/>).

Introduction

Hepatoblastoma (HB) is the predominant pediatric liver tumor, mainly affecting infants under 3 years of age.¹ Although its incidence has increased markedly over the last 30 years, HB is a rare disease (1.8 cases per million children per year).^{2,3} Clinical studies combining chemotherapy and efficient surgical approaches have led to dramatic improvements in outcomes for patients with HB, with a 3-year event-free survival (EFS) above 80%.⁴ However, there are limited treatment options for clinically advanced tumors, with a 3-year EFS of only 34%.⁵ Furthermore, patient survivors can suffer severe and lifelong side effects derived from chemotherapy and immunosuppression. A recent unified analysis from the Children's Hepatic tumors International Collaboration (CHIC) led to the development of a new international clinical staging system for risk

stratification in children with HB.⁶ However, the rarity of the disease has impaired the incorporation of molecular data into this clinical classification. In this context, there is a need to increase our understanding of the biology of this rare tumor and its prognostic determinants to be able to move towards biology-driven precision medicine, which includes biomarkers for therapeutic tailoring.

The origin of HB is largely unknown. Most tumors are sporadic, and their extreme rarity has limited our understanding of their underlying molecular mechanisms. Regarding the genetic alterations identified to date, the most significant are activating mutations of the catenin beta 1 (*CTNNB1*) gene, which encodes β -catenin, in more than 70% of HBs.⁷ β -catenin is a key regulator of cell fate and proliferation during liver development and regeneration. *CTNNB1* mutations in cancer impair the proteosomal degradation of this protein and lead to the constitutive activation of the Wnt pathway.⁸

High-throughput technologies now enable us to identify the molecular subtypes of diverse cancers and their associated oncogenic aberrations. Based on transcriptomic studies, we identified 2 HB subclasses—C1 and C2—that resemble late and early stages of liver development, and a discriminating 16-gene signature.⁹ The recent studies led by French¹⁰ and American¹¹ teams described a third HB subclass not detected by the 16-gene signature. This subclass, called C2B in the paper by Hooks *et al.*,¹⁰ is characterized by increased expression of epithelial-mesenchymal transition markers such as vimentin (*VIM*). A recent pan-cancer analysis showed that HB is the tumor with the lowest rate of somatic mutations (1–7 mutations per tumor genome).¹² However, exome sequencing studies of HB have revealed nuclear factor erythroid 2-related factor 2 (*NFE2L2*), a regulator of critical antioxidant and stress-responsive genes, as the second most mutated gene in ~10% of cases.¹³ In comparison with hepatocellular carcinoma (HCC), the main liver cancer in adults, HB has more than 10-fold fewer mutations. This observation thus suggests that childhood liver tumorigenesis is driven by mechanisms other than DNA mutations, such as epigenetic modifications.¹⁴ To date, genome-wide epigenetic studies on HB are scarce and included a limited number of cases.^{15–17}

Through a high-throughput genomic, transcriptomic and epigenomic study of unprecedented size, we have discovered and validated a profound epigenetic footprint in HB, spanning RNA editing dysregulation to specific DNA methylation profiles linked to strong overexpression of 14q32 genes, Wnt signaling, and a progenitor-like phenotype. Based on our findings, which includes an updated 16-gene signature, we present the first molecular risk stratification of HB, which seeks to improve on the current clinical CHIC risk staging system, and we identify choline kinase alpha (CHKA) as a potential therapeutic target for patients with HB.

Patients and methods

Patients and samples

The study included 113 patients with HB (discovery set: 67 samples, 33 patients; validation set: 92 samples, 80 patients). In total, we analyzed 112 primary tumors, 3 recurrences and 44 paired non-tumor samples (Table S1). The main clinical

Table 1. Main clinical and pathological features of the 113 patients with hepatoblastoma included in the study.

	Discovery set (n = 33)	Validation set (n = 80)
Age, months (median, [range])	16 [1–180]	18 [0.2–204]
Gender (M/F)	20/13	52/28
Serum AFP, ng/ml (range)	341–2,186,461	300–12,299,925
Clinical classification:		
CHIC-HS (VL-L/I/H)	16/4/13	48/7/25
Pre-operative chemotherapy (Y/N, %)	31/2 (94%)	73/7 (91%)
Tumor characteristics:		
PRETEXT stage (I/II/III/IV/n.a.)	2/12/13/6/0	4/31/28/16/1
Vascular Invasion (Y/N, %)	13/20 (39%)	16/64 (20%)
Multifocality (Y/N, %)	12/21 (36%)	19/61 (24%)
Metastasis at diagnosis (Y/N, %)	9/24 (27%)	18/62 (22.5%)
HB histology:		
Epithelial/Mixed/n.a.	17/16/0	54/25/1
MEC: Fetal/Non-Fetal ^a /n.a.	19/13/1	65/14/1
HCN-NOS	2	–
Follow-up, months (mean, [range])	41.76 [1–100]	41.45 [0.2–100]
Outcome: cancer-related deaths or tumor recurrence (Y/N, %)	11/22 (33%)	17/63 (21%)

^aNon-fetal includes crowded fetal, macrotrabecular and embryonal histological subtypes. CHIC-HS, Children's Hepatic tumors International Collaboration-Hepatoblastoma Stratification (VL-L, very low; or low; I, intermediate and H, high risk)⁶; HCN-NOS, hepatocellular neoplasm not otherwise specified; MEC, main epithelial component; n.a., non-available; PRETEXT, PRETreatment EXTent of disease.

characteristics of these patients as well as the pathological and molecular (*CTNNB1* status and C1/C2 classification) features of the tumors are summarized in Table 1.

Molecular profiling

RNA-sequencing (RNA-seq), human transcriptome array (HTA), CytoScan HD and methylation 850K-arrays were performed on the discovery set. The main findings were confirmed in the validation set and 5 human fetal livers. Sample-assay overlap is detailed in Table S1. The omics data generated in this study have been deposited in NCBI's Gene Expression Omnibus¹⁸ and are available through GEO Series accession number GSE132219. Whole-genome sequencing data are available under accession number PRJNA548663 at the Sequence Read Archive of the NCBI.

Additional detailed protocols are provided in supplementary information and CTAT table.

Results

Genomic profiling reveals a recurrent altered sequence of *BLCAP* in HB

RNA-seq data were examined for nucleotide alterations that lead to amino acid changes and fusion transcripts. The study of missense changes found the same point *CTNNB1* mutations as identified by RT-Sanger-sequencing (Table S1), and revealed changes (A/G) in nucleotide (nt) positions 5, 14 and/or 44 of the apoptosis-inducing factor *BLCAP* (bladder cancer-associated protein) transcript in 9 cases of the discovery set (28%) (Fig. 1). *NFE2L2* mutations were found in 3 cases (9%). Analysis of fusion transcripts identified 15 events with perfect alignment in 12 distinct tumors (Table S2). Four of these transcripts were selected and validated in tumor samples and their corresponding patient-derived xenografts (PDX) by RT-PCR-Sanger sequencing (Fig. S1). No additional tumors with these fusion transcripts were

detected in the complete set (total incidence <1%), thereby ruling out their relevance for HB tumorigenesis.

We analyzed the genomic profiling of the same tumors with the high-resolution CytoScan HD array. The recurrent altered chromosomal regions in HB are shown in Fig. 1, confirming previous single-nucleotide polymorphism array- or karyotype-based reports.^{9,11,19} The most frequent chromosomal alterations included broad and focal copy number gains in 1q, 2q, 5p, 6, 7, 8, 12, 13q34, 15q, 17q and 20, and losses in 1p, 4q and 18p11.32 (Fig. S2). The most recurrent, already reported,²⁰ allelic imbalance involved 3.9 Mb of the 11p15 locus (13/32, 41% cases). Other additional recurrent allelic imbalances were found in 1p, 2q, 2p, 3p, 7q, 11p and 17q in 13–22% of the primary tumors, of which the last two, to our knowledge, have not been found in previous studies. Tumors from recurrences or with a HCN-NOS (hepatocellular malignant neoplasms not otherwise specified²¹) histology showed an increased number of chromosomal aberrations (Fig. S2).

Genome-wide dysregulation of RNA editing and *BLCAP* hyperediting in HB

Because *BLCAP* RNA is a highly conserved edited transcript,²² we examined whether the nt 5 A>G substitution (which confers a Y2C change) observed in the RNA-seq data is due to an editing event. RT-PCR-Sanger sequencing revealed that the nt 5 substitution was present only in the RNA and not in the DNA of the tumors (Fig. 2A). This observation strongly points to the dysregulation of RNA editing in the *BLCAP* transcript. The nt 5 editing of *BLCAP* was further confirmed by droplet digital PCR. To this end, we used probes to measure the fractional abundance of wild-type and edited nt 5 of *BLCAP* and found that the latter was 1.85-fold higher in tumor than in non-tumor samples ($p < 0.0001$, Fig. 2B).

These findings on *BLCAP* prompted us to study whether RNA editing is globally disrupted in HB. Genome-wide analysis of RNA changes using RNA-seq data revealed that tumor samples had a lower overall editing index than non-tumor samples in both *Alu* and non-*Alu* regions ($p < 0.0001$, Fig. 2C).

Adenosine deaminases acting on RNA (ADARs) are responsible for converting A to I in nuclear-encoded RNAs, leading to A>G substitutions.²³ We therefore studied whether these enzymes were aberrantly expressed in HB and found a significant overexpression of both *ADAR1* and *ADAR2* genes in tumor compared to non-tumor samples ($p \leq 0.0005$; Fig. 2D). In summary, we discovered an unprecedented dysregulation of global editing and regulatory enzymes and identified *BLCAP* as the first hyperedited gene in HB.

Overexpression of 14q32 genes is a new hallmark of HB

By performing an unsupervised hierarchical clustering of the transcriptomic data, we identified 3 groups of tumors according to the co-clustering study of 12 dendrograms (Fig. S3A). Co-cluster 1 (CC1) and co-cluster 2 (CC2) were enriched in C1 and C2 tumors ($p = 0.001$) whereas the third co-cluster (CC3) composed of C2 tumors, significantly overlapped with the recently identified C2B subclass¹⁰ (Fig. S3B) which had high expression of *VIM* (Fig. S3C). The tumor gene expression profile showed upregulation of the Wnt/ β -catenin pathway, and imprinted and stem cell-related genes (fold change [FC] >2, false discovery rate [FDR] <0.001, Table S3A,B). Among the most strongly dysregulated genes in tumors, as identified by HTA (FC >30, FDR <10⁻⁷), we also found a previously undescribed,

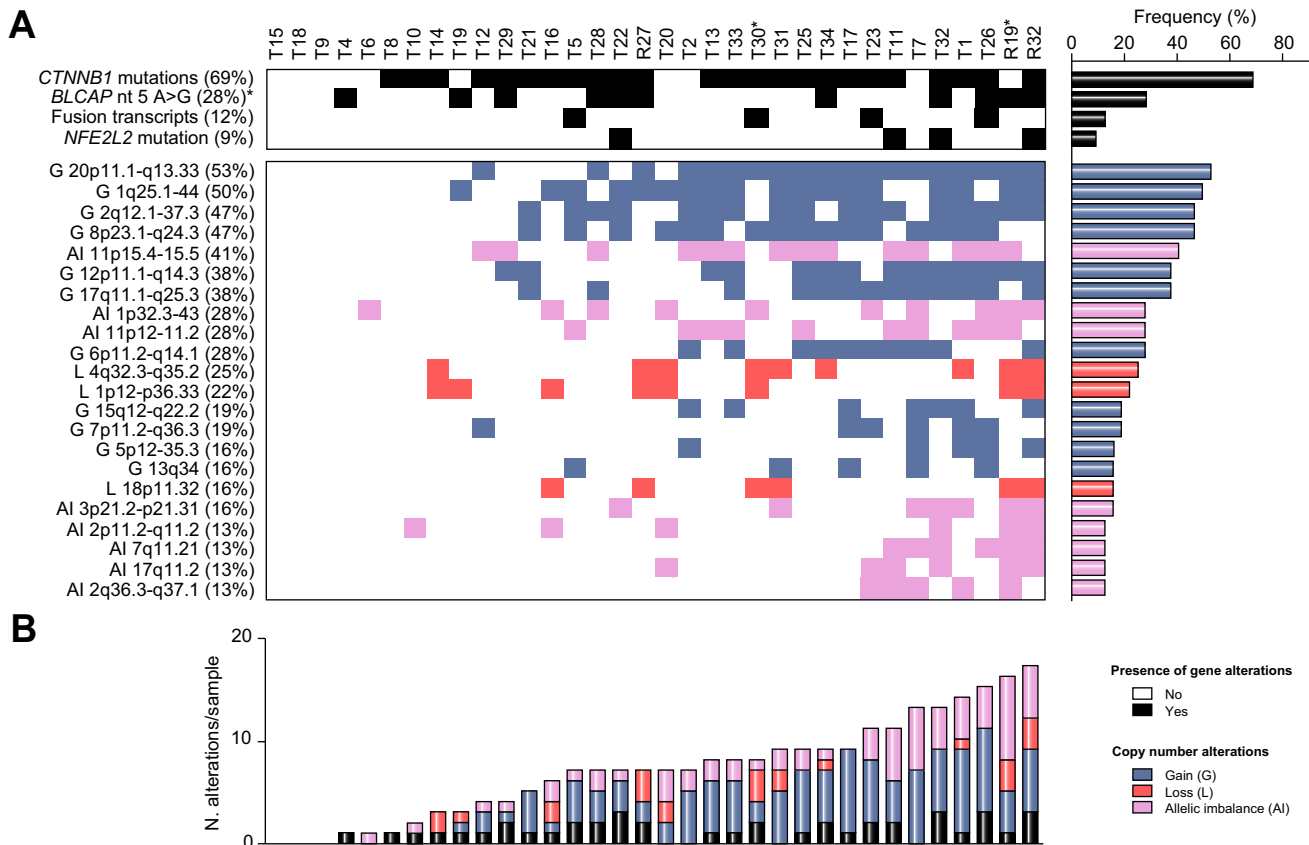


Fig. 1. The genomic landscape of hepatoblastoma. (A) Main gene mutations, fusion transcripts, and chromosomal alterations in the 34 tumor (T) samples from the 32 patients (discovery set) ranked by their frequency (right plot) and considering only 1 sample per patient. *CTNNB1* and *NFE2L2* mutations and *BLCAP* nucleotide 5 change were identified by RNA-seq. Only copy number alterations and allelic imbalances identified by the CytoScan HD array in at least 4 primary tumors are shown. HBs with an HCN-NOS histology are marked with an asterisk. (B) Total number of main aberrations in the above tumor samples. X-axis indicates the individual tumors; Y-axis indicates the number of total gene mutations (black), copy number alterations (gains, blue; losses, red) and allelic imbalances (pink) per sample. HB, hepatoblastoma; HCN-NOS, hepatocellular neoplasm not otherwise specified; R, recurrence; RNA-Seq, RNA sequencing.

highly upregulated 330 kb region within the *DLK1* (delta-like non-canonical notch ligand)-*DIO3* (iodothyronine deiodinase 3) locus, spanning from 14q32.2 to q32.31, called 14q32 henceforth (Fig. 3A, see Fig. S4A,B for more details). This is an imprinted region with a key role in human development and cancer.^{24,25} It contains more than 100 transcripts, including *DLK1* (a well-known hepatoblast marker highly expressed in HB^{9,26}), *MEG3* and *MEG8* (2 maternally expressed non-coding genes), small nucleolar RNAs of the C/D box family (namely *SNORD113* and *SNORD114*), and the largest microRNA cluster in the human genome (Fig. 3A). Tumor overexpression of 14q32 genes was further validated by gene set enrichment analysis (GSEA) (Fig. 3B, Table S4).

Hierarchical clustering based on the gene expression profile of all the genes localized at 14q32 showed 2 main groups of tumors, thus revealing variability among HBs (Fig. 3C). This heterogeneity was observed at the level of tumor/non-tumor expression of 14q32 genes and in the number of overexpressed genes (Fig. S4C). Among these genes, 4 (*DLK1*, *MEG3*, *SNORD113-3*, *SNORD114-22*) were selected to classify tumors on the basis of the degree of 14q32 gene expression (strong/moderate), and they are referred to as the 14q32-gene signature hereafter (Fig. S4D). Strikingly, the resulting 14q32 classification was also associated with mutations in the Wnt/ β -catenin pathway

($p < 0.0001$, Fig. 3C). We assessed the mRNA expression of 14q32 in the validation set and confirmed the overexpression of 14q32 genes. Its correlation with the Wnt/ β -catenin pathway activation was also confirmed in the validation set by measuring *LGR5*, a well-known wnt/ β -catenin target gene²⁷ (Fig. S5). Moreover, the study of fetal liver samples also indicated an elevated expression of 14q32 genes, thereby reinforcing the idea that HB recapitulates pathological and molecular features of developing livers.^{9,28}

To gain insight into the possible mechanisms conferring strong 14q32 gene expression in HB, we examined the 14q32 region at the genomic and epigenomic level. Since 14q32 gene overexpression has previously been linked to adeno-associated virus integration in this locus and hepatocarcinogenesis,^{29,30} we used whole genome sequencing to search for viral integration in a tumor with a strong 14q32-gene signature. No viral integration site was detected (Table S5, Fig. S6). Neither did the CytoScan HD array reveal focal chromosomal rearrangements. In contrast, the comparison of tumor and non-tumor methylation profiles using the 850K-array identified 32 significant differently methylated CpGs localized at the 14q32 locus with predominant tumor DNA hypomethylation (FDR < 0.05), specifically, the methylation levels of a CpG (cg02412314) localized within the intragenic *MEG3* region

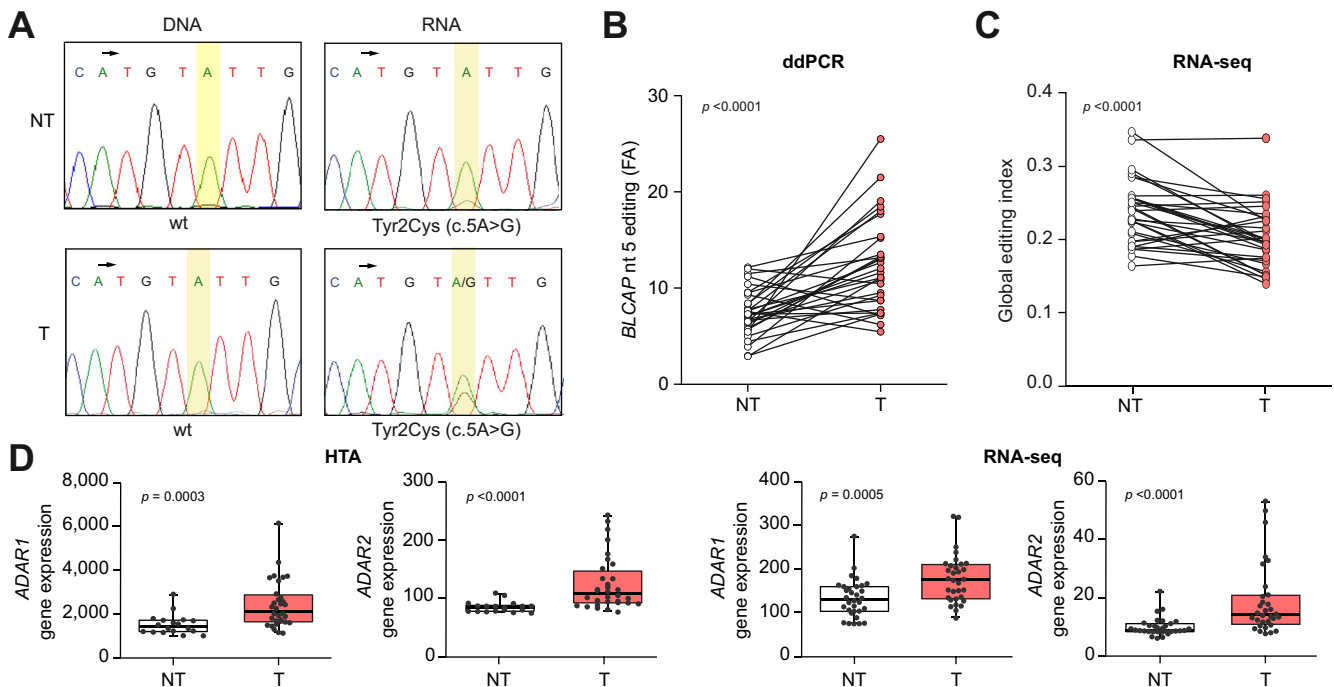


Fig. 2. Dysregulation of RNA editing in hepatoblastoma. (A) Chromatogram of DNA and RNA Sanger sequences of the *BLCAP* gene in tumor (T) and non-tumor (NT) samples of a representative case with RNA editing of nucleotide 5 (highlighted in yellow). The black arrow indicates the ATG start codon. (B) FA of nucleotide 5 edited vs. non-edited *BLCAP* assessed by ddPCR in the 31 paired T and NT samples (discovery set) for which RNA was available (paired *t* test). (C) Global editing index in the 32 cases of the discovery set determined by RNA-seq (paired *t* test). (D) Gene expression of *ADAR1* and *ADAR2* genes in T and NT samples (Mann-Whitney *U* test). HTA plot includes data of 18 NT and 32 T samples; RNA-seq plot includes data of 32 NT and 32 T samples. Gene expression is given in normalized arbitrary units (HTA array) or counts (RNA-seq). *BLCAP*, bladder cancer associated protein; ddPCR, droplet digital PCR; FA, fractional abundance; HTA, human transcriptome array; RNA-seq, RNA sequencing.

showed a strong correlation with the mean gene expression of the 14q32 region ($r = -0.61$, $p < 0.0001$, Fig. 3D). Interestingly, tumors with a strong 14q32-gene signature displayed lower methylation of the 32 CpGs than tumors with a moderate signature ($p = 0.0082$, Fig. 3E). Moreover, fetal liver samples showed the lowest levels of 14q32 methylation compared with tumor samples (Fig. 3E).

Identification of two distinct epigenetic profiles in HB

Next, we used the 850K-array data to extend our methylation study to the complete genome. Principal component analysis of the methylation data showed that tumor samples were clearly distinct from non-tumor samples (Fig. 4A). In general, tumors were characterized by genome-wide DNA hypomethylation ($p < 0.0001$). The supervised analysis comparing tumor and non-tumor samples identified 30,165 differently methylated CpGs regulating 7,234 genes ($|\Delta\beta| > 0.20$, FDR < 0.0001), including hypermethylation of the *RASSF1* promoter.³¹ Using HTA and RNA-seq to associate these data with gene expression, we found 21 hypermethylated ($\Delta\beta > 0.20$, FDR < 0.0001) genes in tumors with concomitant reduced gene expression (FC < -2 , FDR < 0.05) (Table S6). Among them, we recognized genes endowed with tumor suppressor functions such as *AKR7A3*,³² *EDNRB*,³³ *ESRP2*,³⁴ *PEMT*³⁵ and *PER3*.³⁶

The unsupervised analysis showed separate clusters of tumor and non-tumor samples ($p < 0.0001$). The epigenetic clustering also disclosed two distinct tumor clusters, which we called Epigenetic-Cluster A and Epigenetic-Cluster B (Epi-CA and Epi-CB) (Fig. 4B) which were not associated with the 16-gene C1/C2

classification⁹ ($p = 0.6882$) but were strongly associated with our CC1/CC2/CC3 transcriptomic co-clusters ($p \leq 0.0005$) and with the Hooks signature¹⁰ ($p < 0.005$). Moreover, the Epi-CB cluster, which was enriched with tumors of the C2 subtype, exhibited constitutive activation of Wnt/ β -catenin signaling ($p = 0.0391$) and a strong 14q32-gene signature ($p = 0.0010$) (Fig. 4B). The study of the methylation profiles between the 2 tumor clusters revealed that Epi-CB tumors had a sharp global hypomethylation compared to Epi-CA tumors in all epigenomic structures, except for CpG islands, which were hypermethylated (Fig. 4C). We next studied the impact of this specific CpG island hypermethylation on the transcriptome of Epi-CB tumors and identified *KLF6*, *ITGB3*, *NFIC*, *TRANK1* and *TSPYL5* as possible tumor suppressor genes, as the hypermethylation of their CpG islands ($\beta > 0.2$ and FDR < 0.0001) was associated with a switch-off of their expression (RNA-seq/HTA: FC < -2 and FDR < 0.001 , Fig. 4D). Next, we sought to investigate whether the dysregulation of methylation observed in HB was associated with changes in the expression of the enzymes regulating DNA methylation. The expression of tet methylcytosine (*TET*) family genes — specifically *TET1* and *TET3* — involved in DNA demethylation, was significantly higher in tumors compared to non-tumor tissue and correlated with the degree of hypomethylation (Fig. S7A). Therefore, Epi-CB tumors with strong global hypomethylation had significantly higher levels of *TET1* and *TET3* than Epi-CA tumors ($p < 0.0025$). Similarly, the expression levels of DNA methyltransferases (*DNMT1*, *DNMT3A* and *DNMT3B*) were higher in tumors than non-tumor samples ($p < 0.0001$) and mainly in Epi-CB tumors characterized by CpG island methylation. Moreover, expression of DNMTs was

also correlated with high level of CpG island methylation (Fig. S7B).

As we reported that C1/C2 subtypes resembled late and early liver developmental stages,⁹ we examined whether the 2 distinct tumor methylation profiles also mimicked the different methylation profiles of adjacent non-tumor and fetal liver samples based of different ages. In line with our previous findings,⁹ we observed that the global methylation value of Epi-CB tumors, enriched with C2 tumors, was similar to that of early embryonal/fetal phases of liver development at 8.4 ± 7.7 weeks of gestation, while the Epi-CA tumors, enriched with C1 and C2B tumors, had a global methylation value similar to that of late fetal or postnatal liver phases at ~5 weeks after birth (Fig. 4E).

Molecular risk stratification of HB

To address the relevance of our molecular findings in the clinical setting, we studied their association with clinical parameters in the whole set of 113 patients (77% *CTNNB1* mutations, 4% *NFE2L2* mutations, 25% *BLCAP* nt 5 hyperediting, 63% strong 14q32-gene signature, 33% Epi-CB, and 44% C2; Table S7). Moreover, we measured *VIM* expression in order to determine its impact on our previous 16-gene signature⁹ and defined an updated 16+*VIM*-gene signature that classified the C2 tumors as either C2B¹⁰ (11%) or C2-Pure (34%) on the basis of high or low levels of *VIM*, respectively. The association of these molecular features with clinical data revealed that the losses of chromosome 4q or 18 and the 17q11.2 allelic imbalance (where the tumor suppressor neurofibromin 1, *NF1*, is localized) were associated with poor prognostic parameters (see more details Table S8). Moreover, patients with tumors with a strong 14q32-gene signature or classified as Epi-CB or C2-Pure had a poorer outcome than those with tumors with a moderate 14q32-gene signature or classified as Epi-CA or C1/C2B (Fig. S7). On the contrary, *CTNNB1*, *VIM* and *BLCAP* editing were not associated with any parameter of poor outcome.

Next, based on the presence of the novel biomarkers of poor prognosis, we defined the first molecular risk stratification of HB (MRS-HB) (Fig. 5A). The low-risk category (MRS-1) included tumors without any biomarker of poor prognosis (i.e., a moderate 14q32-gene signature and Epi-CA) and was enriched for wild-type *CTNNB1* tumors ($p = 0.012$). Tumors in the intermediate-risk category (MRS-2) were defined by having only one biomarker (i.e., a strong 14q32-gene signature or Epi-CB), whereas those in the high-risk category (MRS-3) had two poor prognostic biomarkers (i.e., a strong 14q32-gene signature and Epi-CB) and were enriched for *NFE2L2* mutations ($p = 0.005$). Kaplan-Meier survival curves showed that the 3-year EFS was 91%, 82%, and 52% for patients with MRS-1, MRS-2 and MRS-3 tumors, respectively ($p < 0.0001$, Fig. 5B). To identify the most aggressive tumors, we integrated the 16+*VIM*-gene signature to the MRS and subdivided the high-risk category (MRS-3) into MRS-3a (C1 and C2B) and MRS-3b (C2-Pure); we defined the latter as a very high-risk category, which was associated with a 3-year EFS of only 37% ($p < 0.0001$, Fig. 5B). Importantly, the multivariate analysis indicated that this novel risk stratification based on molecular parameters is an independent prognostic factor of the current clinical CHIC hepatoblastoma stratification⁶ (Fig. 5C,D). Accordingly, the combination of clinical and molecular staging systems (Fig. 5E) resulted in improved performance at discriminating low- and high-risk patients ($p < 0.0001$, Fig. 5F).

CHKA as a new therapeutic target for intermediate and high-risk HBs

To identify therapeutic targets for aggressive HBs, we performed a supervised analysis comparing the 3 main molecular risk categories. Among the 392 differentially expressed genes (FDR < 0.0001 , Table S9), we observed overexpression of 14q32 transcripts (*DLK1*, *MEG3*, *SNORD113-4* and *SNORD114-13*) and liver progenitor markers (*GPC3*, *KRT19*, *AFP*, *EPCAM*) in tumors belonging to the high-risk category (MRS-3) compared to tumors in the low-risk (MRS-1), and to a lesser extent, to those in the intermediate-risk (MRS-2) categories. The most widely overexpressed coding gene in high-risk and intermediate-risk tumors was *CHKA* (Table S9, Fig. 6A), the main regulator of the biosynthesis of phosphatidylcholine via the CDP-choline pathway, which plays a key role in regulating cell growth and carcinogenesis.³⁷ The differential expression of *CHKA* between MRS categories (Fig. 6B), as well as proliferation (Ki67), 14q32 (*DLK1*) and liver progenitor (EPCAM, *GPC3*, *KRT19*, *AFP*) markers was also seen by immunohistochemistry (IHC) in 20 tumors (Fig. S9).

To address whether *CHKA* could be used as a therapeutic target for HB, we tested the anti-tumoral ability of two *CHKA* inhibitors (MN58b and TCD-717)³⁸ at growing concentrations (2–8 μ M) in two HB cell lines, HepG2 and Huh6. Both *CHKA* inhibitors exerted a dose-dependent reduction of cell viability in the two cell lines ($p = 0.0005$ and $p < 0.0001$, respectively) (Fig. 6C). Similarly, MN58b and TCD-717 completely inhibited colony formation in HepG2 and Huh6 cells ($p < 0.0001$, Fig. 6C). We also investigated the anti-tumoral effects of silencing *CHKA* gene expression via small interfering RNA in the Huh6 cell line, which has the lower expression of this enzyme. After depleting *CHKA* by ~4-fold, cell viability of Huh6 cells was reduced by ~15% ($p < 0.0001$; Fig. 6D).

Next, we assessed the *in vivo* anti-tumor effects of *CHKA* inhibition using MN58b in a PDX established from a high-risk HB whose *CHKA* mRNA and protein levels are representative of intermediate and high-risk tumors (Fig. S10). Interestingly, *CHKA* inhibition fully abrogated tumor growth throughout treatment compared with the control arm (vehicle) ($p = 0.028$, Fig. 6E). The IHC study revealed that MN58b-treated tumors showed a significantly lower proliferation rate, as determined by CCND1 (cyclin D1) and Ki67, as well as more commonly reverting from the tumor progenitor-like phenotype than vehicle-treated PDXs (Fig. S11). In addition, MN58b-treated tumors showed a significant increase of necrotic areas and a trend of having higher levels of the active form of caspase-3 than tumors in the control arm (Fig. S12).

Discussion

Through comprehensive molecular profiling, we herein identified an unprecedented widespread epigenomic footprint of HB that includes RNA editing dysregulation, overexpression of mainly non-coding genes in the oncogenic 14q32 *DLK1-DIO3* locus, and two distinct epigenomic tumor profiles that associate with the transcriptomic C1/C2/C2B subtypes previously defined by Cairo-Armengol *et al.*⁹ and Hooks *et al.*¹⁰ The integration of these epigenetic hallmarks together with an updated 16-gene signature allowed us to develop the first molecular risk stratification of HB, which improves on current clinical patient risk classification, and to identify *CHKA* as a potential therapeutic target for patients with HB.

Our study revealed a genome-wide dysregulation of RNA editing in HB for the first time. RNA editing is a widespread

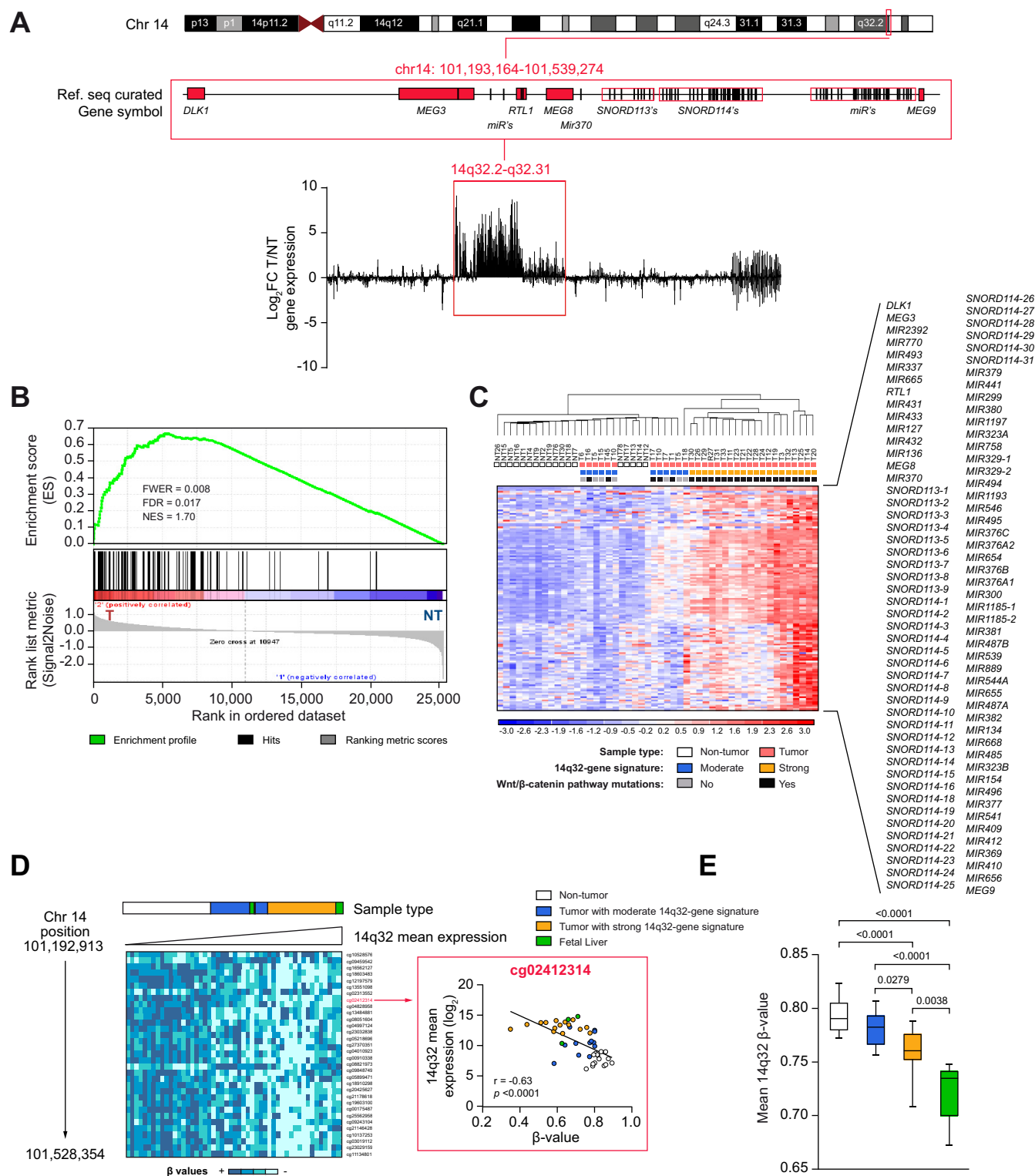


Fig. 3. Overexpression of genes of the 14q32 *DLK1-DIO3* locus is a hallmark of hepatoblastoma. (A) Top, scheme of chromosome 14 in which the overexpressed 14q32 region in HB is marked with a red square. Middle, detail of the overexpressed 14q32 genes of the *DLK1-DIO3* locus. Bottom, the X-axis indicates the gene chromosomal localization from 14q32.13 to 14qter. Y-axis is the mean tumor (T)/non-tumor (NT) FC of the genes of the 14q32 region present in the HTA array in normalized arbitrary units. The box and whiskers represent the 25th to 75th percentiles and \pm min to max values, respectively, of log₂ gene expression of 32 tumors. (B) GSEA enrichment plot using the 96 genes of the HTA array out of the total of 101 genes presenting the 14q32 region (chr14:101193164-101539274) based on the Genome Browser Database hg19. (C) Unsupervised clustering and heatmap of the 133 HTA array probesets (right) at the overexpressed 14q32 chromosomal region of 32 T and 18 NT samples. (D) Left, heatmap of the methylation degree of the 32 significant CpGs (FDR <0.05) localized in the overexpressed 14q32 region. The color range in the heatmap indicates the methylation degree of each CpG. Right, correlation between mean gene expression of 14q32 genes (133 probesets) and the methylation (β -value) of the most significant 14q32 CpG, which is localized in a *MEG3* intronic region (Spearman test). (E) Mean

epigenetic mechanism that confers specific nucleotide changes on RNA transcripts without altering the sequence of genomic DNA; thereby contributing to transcriptomic diversity in normal but also cancer cells.³⁹ The functional impact of RNA editing on cell biology ranges from protein recoding to alterations in alternative splicing, miRNA specificity and RNA stability.⁴⁰ Herein, in HBs, we identified global hypoediting, specific hyperediting of *BLCAP*, a highly conserved gene with potential tumor suppressor functions,^{22,41,42} and also an imbalance in the expression of ADAR enzymes; the main regulators of RNA editing.²³ Our findings agree with the observed dysregulation of RNA editing across different cancer types with over- and under-editing patterns relative to non-tumor samples.^{39,40,43} Similar to our data, global RNA editing dysregulation in cancer has also been associated with the hyperediting of key genes.⁴⁰ In that regard, increased hyperediting of *BLCAP* has already been reported in HCC⁴⁴ and to a minor degree in brain, cervical, oral cavity and lung tumors.^{45,46} Previous investigations revealed that *BLCAP* editing could affect the functions of several binding proteins such as RB⁴⁷ or STAT3⁴⁶; thereby, influencing proliferation and apoptotic signaling pathways. In HCC, experiments performed in SMMC_7721 and Focus liver cancer cell lines revealed that nt 5 editing confers a growth advantage, modulating the activation of AKT/mTOR signaling.⁴⁴ Overall, our study reveals an unexplored field related to RNA editing in HB. Future studies will need to clarify the functional effects of *BLCAP* editing in these tumors.

The second epigenetic alteration we observed pertains to the pronounced overexpression of mainly non-coding genes localized in a small 14q32 region of the *DLK1-DIO3* locus in almost all the HBs examined and that is highly correlated with their degree of methylation. In addition to *DLK1*, a well-known hepatoblast marker overexpressed in HB,^{9,26} this locus is characterized by a cluster of imprinted genes whose altered dosage is associated with developmental defects and liver oncogenesis.^{24,29,48} Interestingly, the expression of the *DLK1-DIO3* locus has been proposed as a marker of induced pluripotent stem cells, thereby supporting its role in early development.⁴⁹ In agreement with these previous studies, our data suggest a fine-tuned regulation of the 14q32 region during liver development, since its transcripts were highly expressed in fetal livers but strongly repressed in postnatal ones. In that regard, we found that HBs present an aberrant expression of 14q32 genes, an observation that supports the notion that these genes are involved in hepatic tumorigenesis. The oncogenic role of 14q32 genes in the liver was initially identified through research into the mechanisms involved in the spontaneous development of HCC in mice treated with adeno-associated viruses (AAVs).²⁹ Moreover, the gene-targeting frequency of this locus by AAVs was shown to be sufficient to initiate multiple foci of HCC in mice characterized by *Dlk1-Glt2* overexpression linked to CpG hypomethylation.⁵⁰ In agreement with these experimental data, 2 independent studies reported the overexpression of 14q32 genes in a subset of 6–19% of patients with HCC and poor prognosis.^{48,51} In line with these studies on HCC, we found that the overexpression of 14q32 genes

is linked to high expression of liver progenitor cell markers and Wnt/ β -catenin targets and that it influences the survival of patients with HB. Collectively, our study pinpoints the overexpression of 14q32 genes of the *DLK1-DIO3* locus as a novel oncogenic hallmark of HB.

Dysregulation of DNA methylation might be considered a third epigenetic hallmark of HB. DNA methylation plays an important role in cell differentiation and cancer, influencing the regulation of gene expression networks.^{52,53} The genome-wide DNA hypomethylation that we found in HB is consistent with the findings of previous reports.^{15–17} As a novelty, we discovered 2 distinct epigenetic profiles in HB based on the degree of DNA hypomethylation and CpG island hypermethylation. We also associated these epigenomic traits with the previously defined C1/C2/C2B molecular subclasses.^{9,10} Our results demonstrate how the interplay between the epigenome and the transcriptome determines distinct tumor molecular entities. Moreover, we investigated the impact of CpG island hypermethylation, an additional level of epigenetic dysregulation in Epi-CB tumors belonging mainly to the C2 subtype, and identified novel tumor suppressor candidates whose expression was strongly repressed in aggressive HB, which could be explored in further functional studies.

In an attempt to translate our findings into the clinical setting, we propose the first molecular risk stratification system, called MRS, for HB. This system is based on the presence of the 2 novel prognostic biomarkers identified in the current study (*i.e.* 14q32-gene signature and Epi-CA/B). Of note, the prognostic impact of the MRS is improved by incorporating the updated 16-gene signature described here, which includes *VIM* expression, to distinguish the recently reported C2B subclass.¹⁰ The benefit of the MRS compared to our previously published 16-gene signature is that it is able to better differentiate patients according to their prognosis. This could be explained by the fact that MRS integrates both epigenetic and transcriptomic classifiers, providing a better representation of the molecular complexity of HB. Moreover, like the clinical CHIC hepatoblastoma stratification,⁶ the integration of multiple molecular prognostic factors may have an additive effect in terms of risk prediction. By combining the clinical CHIC and the molecular MRS systems, we have been able to further improve patient risk prediction. In this regard, our findings highlight the importance of incorporating molecular factors into the clinical setting, thereby facilitating future precision medicine. The main limitations of the current study lie in the use of a retrospective cohort of patients treated with different chemotherapeutic protocols and the study of post-chemotherapy specimens. Thus, the implementation of our findings into the clinical setting requires a further validation in diagnostic biopsies from homogeneously treated patients and probably the definition of a new algorithm integrating clinical and molecular parameters; the prospective cohort of patients enrolled in the ongoing Paediatric Hepatic International Tumour Trial (PHITT, NCT03017326) provides a unique opportunity to conduct such validation.

Finally, we identified CHKA as a novel potential therapeutic target for HB patients. CHKA, a key gene for membrane

methylation levels (β -value) of all 568 CpGs localized in the 14q32 region in the 3 different sample types (NT, $n = 19$; T with moderate and strong 14q32-gene signature, $n = 12$ and $n = 15$, respectively; fetal liver samples, $n = 5$). p values were calculated using the ANOVA test with the Tukey post-test. FC, fold change; FDR, false discovery rate; GSEA, gene set enrichment analysis; HB, hepatoblastoma; HTA, human transcriptome array.

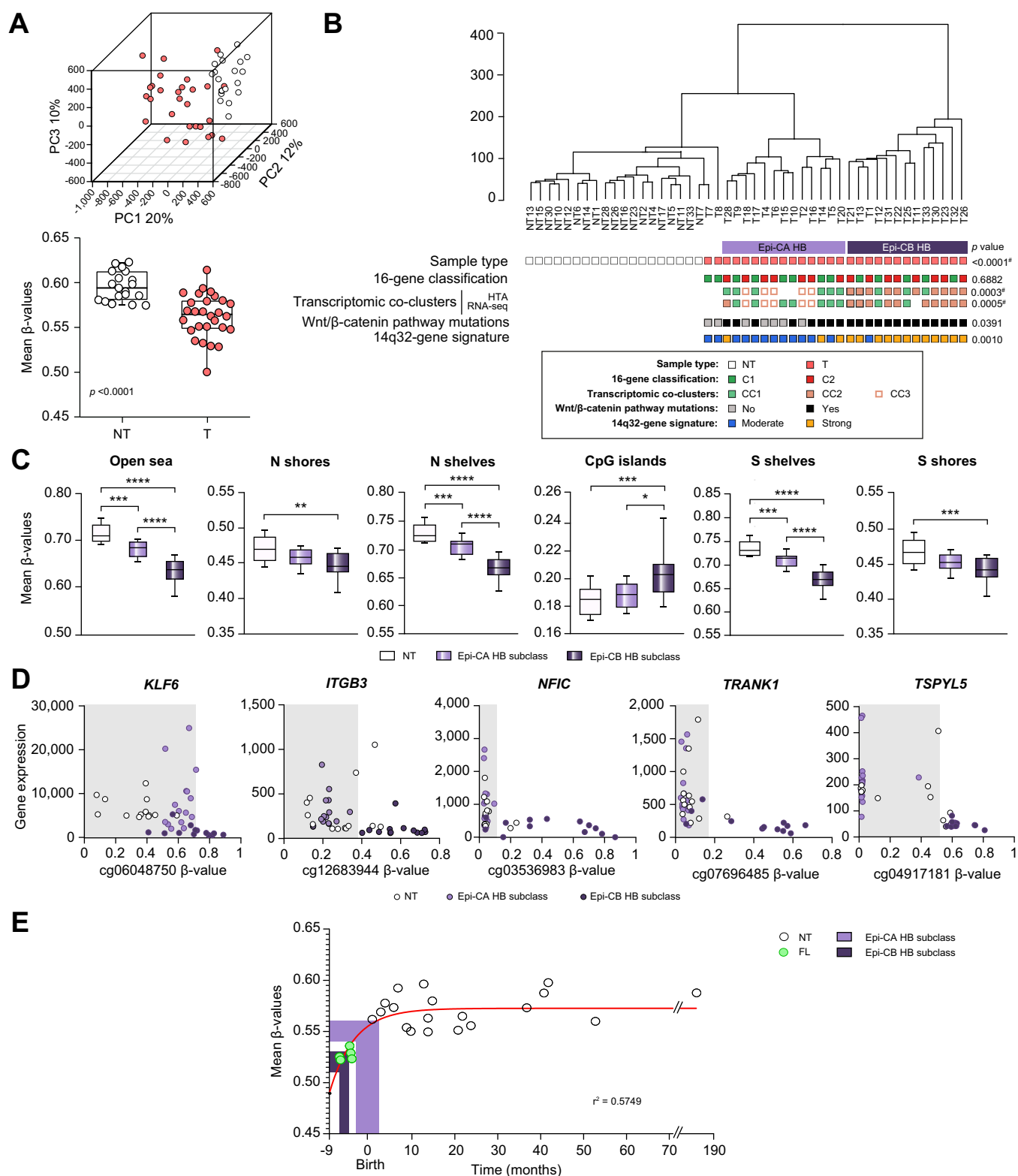


Fig. 4. Identification of two epigenetic hepatoblastoma subtypes resembling the transcriptomic co-clusters. (A) Top, principal component analysis of tumor (T, n = 28) and non-tumor (NT, n = 19) samples using normalized methylation data of the 685,375 CpGs of the 850K-array obtained after filtering those probes containing single nucleotide polymorphisms. Bottom, mean global methylation levels (β -value) of the same samples (unpaired *t* test). The box and whiskers represent the 25th to 75th percentiles and \pm min to max values, respectively. (B) Representative unsupervised clustering (Euclidean Ward method) of same CpGs used for the principal component analysis. *p* values indicate the associations between the listed molecular features and the 2 tumor epigenetic clusters, Epi-CA and Epi-CB. *p* values were calculated using Fisher's exact and χ^2 tests. (C) Methylation levels of the epigenetic substructures in NT (n = 19), Epi-CA (n = 13) and Epi-CB (n = 13) tumors. The box and whiskers represent the 25th to 75th percentiles and \pm min to max values, respectively. *p* values were calculated using the ANOVA test with the Tukey post-test (**p* < 0.05; ***p* \leq 0.001; ****p* < 0.0001). (D) Representation of the 5 most strongly repressed genes by CpG island

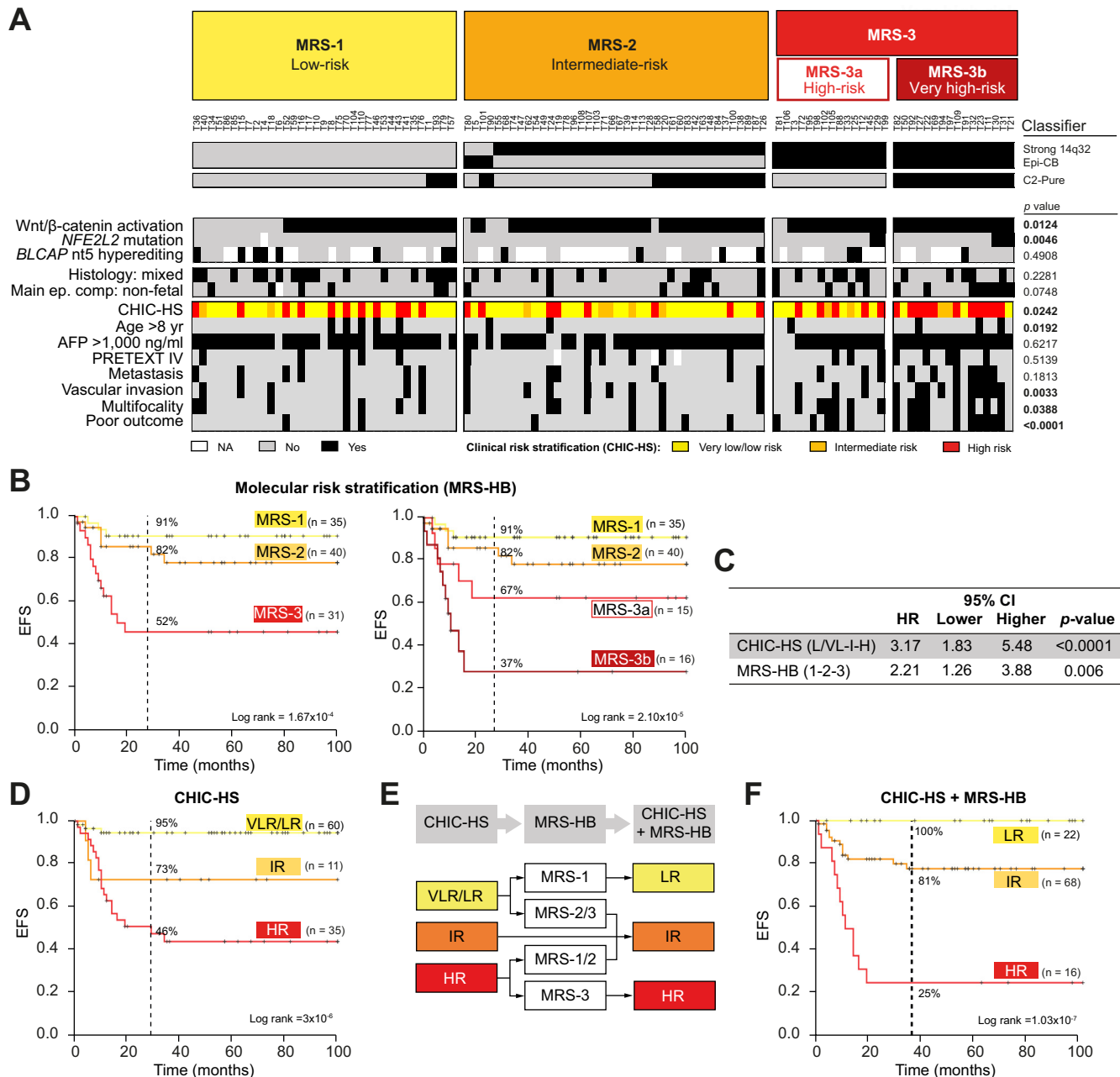


Fig. 5. Molecular Risk Stratification of Hepatoblastoma (MRS-HB). (A) Top, representation of the MRS-HB categories for the 106 patients from which all biomarkers could be assessed. Patient stratification was based on transcriptomic and epigenetic classifiers (right): 14q32- and 16+VIM-gene signatures and epigenomic Epi-CA/Epi-CB classification. Bottom, main genomic, pathologic and clinical features and their association with the MRS (right, Chi-Square test). (B) EFS Kaplan-Meier plots of the same patients stratified according to the MRS-HB into 3 (left) or 4 (right) categories. Vertical line indicates 3-year EFS probability (in %). (C) Multivariate Cox regression analysis comparing MRS with clinical CHIC-HS Stratification.⁶ (D) EFS Kaplan-Meier plots of the same patients with HB classified following the CHIC-HS stratification (VLR/L, Very Low and Low; L, Low; I, Intermediate; H, High risk). (E) Scheme used to combine CHIC-HS and MRS-HB classifications. (F) EFS Kaplan-Meier plots of the 106 patients with HB classified by combining clinical and molecular risk stratification systems. CHIC-HS, Children's Hepatic tumors International Collaboration-Hepatoblastoma Stratification; Epi-CA/B, Epigenetic-Cluster; EFS, event-free survival; HB, hepatoblastoma; HR, hazard ratio; MRS, Molecular Risk Stratification.

hypermethylation in Epi-CB tumors (RNA-seq/HTA criteria: FC <-2 and FDR <0.001; 850K-array criteria: β >0.2 and FDR <0.0001). The X-axis indicates methylation levels of the most hypermethylated CpGs islands for each gene and the Y-axis the linear gene expression levels (HTA). The grey shadow indicated the low CpG island methylation levels associated to high gene expression. (E) Global methylation levels (Y-axis) of 19 NT (white dots) and 5 fetal liver samples (FL; green dots) at different gestational and postnatal ages (X-axis). The light and dark purple shadows indicate the 25th and 75th percentiles of the methylation levels of Epi-CA and Epi-CB tumors, respectively, and their extrapolation over time. Note the plateau of methylation levels at ~12–24 months of age. Red, exponential curve. Epi-CA/B, Epigenetic-Cluster A/B; FC, fold change; FDR, false discovery rate; HTA, human transcriptome array; *ITGB3*, integrin subunit beta 3; *KLF6*, Kruppel like factor 6; *NFIC*, nuclear factor I C; *TRANK1*, tetratricopeptide repeat and ankyrin repeat containing 1; *TSPYL5*, TSPY like 5.

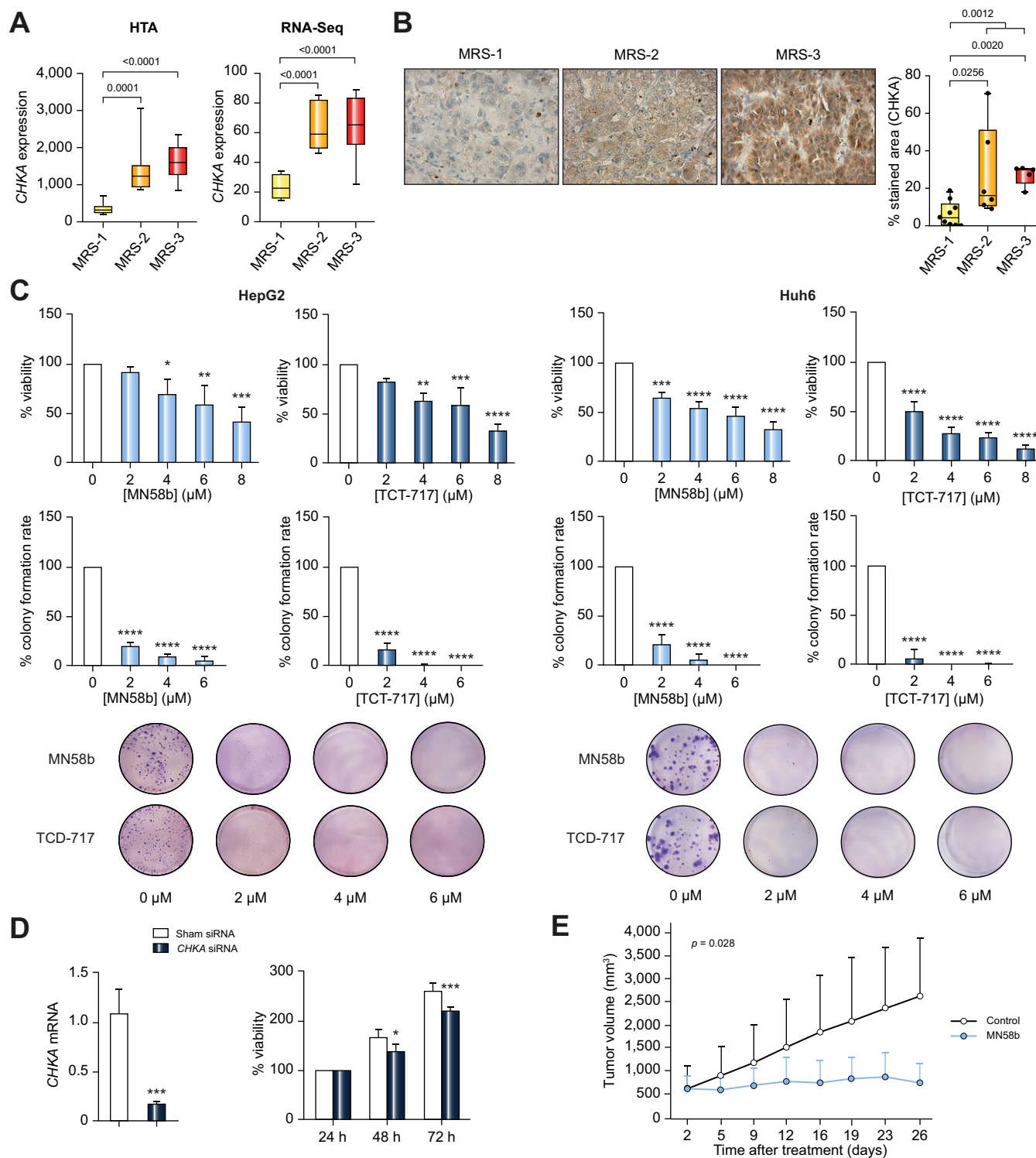


Fig. 6. The effect of inhibition of CHKA in hepatoblastoma. (A) CHKA gene expression assessed by HTA and RNA-seq in the different risk molecular risk categories (MRS-1, n = 11; MRS-2, n = 8; MRS-3, n = 13)[†]. (B) Left, Images of CHKA immunostaining for representative tumors according to MRS. Right, quantification of stained areas of CHKA immunohistochemistry in formalin-fixed paraffin-embedded tumor samples (MRS-1, n = 9; MRS-2, n = 6; MRS-3, n = 5)[†]. (C) Cell viability assay (MTT)[†] (top) and colony-formation assay[†] (middle) of HepG2 (left) and Huh6 (right) cells treated by at different concentrations of CHKA inhibitors (MN58b and TCD-717) for 48 h. 0 μM of TCD-717 was prepared with DMSO at the same concentration of 8 μM of MN58b. Representative colony-formation assay images of the different conditions (bottom). Data given are from a minimum of 3 independent experiments. *p* values were calculated vs. control. (D) CHKA gene expression[‡] assessed by RT-qPCR of control (Sham siRNA, white) and CHKA knock-down (CHKA-siRNA, black) in Huh6 cells. Cell viability assay (MTT) assay[‡] of the same cells at different time points of culture. Data given are from four independent experiments. *p* values were calculated vs. control. (E) Tumor growth curve of a PDX established from a high-risk tumor (MRS-3, case T50) following intraperitoneal injection of vehicle (phosphate buffered saline, control; n = 5) or 3 mg/kg/day of CHKA inhibitor (MN58b; n = 6). *p* values was calculated using the two-tailed *t* test with Welch's correction

biosynthesis, is overexpressed in different neoplasms such as breast, lung, prostate, and HCC.^{54–57} The complete abrogation of tumor growth that we observed *in vitro* and *in vivo* using two HB cell lines and a PDX model is achieved by an inhibition of proliferation and induction of cell death. Of note, CHKA has been proposed as a therapeutic target in different tumor types^{57,58} and TCD-717 has already been evaluated in a phase I clinical trial (NCT01215864) in advanced solid tumors. Our findings thereby support further attention to CHKA inhibition as a potential therapy for patients with HB.

The similarities observed between HB (*i.e.* BLCAP hyperediting, 14q32 locus overexpression, CHKA overexpression) and HCC also point to common underlying mechanisms between the main hepatic tumors in childhood and adulthood, shedding light on overlapping molecular mechanisms and common therapeutic approaches.

In summary, our data provide novel epigenetic insights into HB and establish the rationale to advance towards precision medicine by identifying new biology-driven therapies and incorporating molecular data into patient stratification.

Abbreviations

AAV, adeno-associated viruses; BLCAP, bladder cancer associated protein; CHIC, Children's Hepatic tumors International Collaboration; CHIC-HS, CHIC-Hepatoblastoma Stratification; CHKA, choline kinase alpha; ddPCR, droplet digital PCR; EFS, event-free survival; Epi-CA/B, Epigenetic-Cluster A/B; FA, fractional abundance; FC, fold change; FDR, false discovery rate; GSEA, gene set enrichment analysis; HB, hepatoblastoma; HCC, hepatocellular carcinoma; HCN-NOS, hepatocellular neoplasm not otherwise specified; HR, hazard ratio; HTA, human transcriptome array; *ITGB3*, integrin subunit beta 3; *KLF6*, Kruppel like factor 6; MEC, main epithelial component; MRS, Molecular Risk Stratification; *NFIC*, nuclear factor I C; *NF1*, neurofibromin 1; PDX, patient-derived xenograft; PRETEXT, PRETreatment EXtent of disease; RNA-seq, RNA sequencing; RT-qPCR, reverse transcription quantitative PCR; siRNA, small interfering RNA; *TRANK1*, tetra-tricopeptide repeat and ankyrin repeat containing 1; *TSPYL5*, TSPY like 5.

Financial support

This article was possible thanks to the inputs from the Instituto de Salud Carlos III, ISCIII (PI09/00751, PI10/02082, PI13/02340). The project has received funding from the European Union's Horizon 2020 research and innovation programme under grant agreement No 668596 (ChiLTERN) and grant agreement No 826121 (iPC). JCR is supported by the Catalan Agency for Management of University and Research Grants (AGAUR, 2019 FI_B01024). LT is supported by an Accelerator Award (CRUCK, AECC, AIRC) (HUNTER, C9380/A26813). DS is supported by the Gilead Research Scholar in Liver Disease. JML is supported by the European Union's Horizon 2020 research and innovation programme (HEPCAR, 667273-2), Institució Catalana de Recerca i Estudis Avançats (ICREA), U.S. Department of Defense (CA150272P3), an Accelerator Award (CRUCK, AECC, AIRC)

(HUNTER, C9380/A26813), National Cancer Institute, Tisch Cancer Institute (P30-CA196521), Samuel Waxman Cancer Research Foundation, Spanish National Health Institute (SAF2016-76390) and AGAUR (SGR-1358). CA and MRS were supported by Ramón y Cajal (RYC-2010-07249) and Miguel Servet (CP14/00021) programs of the Ministry of Science and Innovation of Spain and ISCIII, respectively. CA, MRS and MS received funding from CIBERehd (CB06/04/0033) and AGAUR (2017-SGR-490). IGTP is a member of the CERCA network of institutes. The funders had no role in study design, data collection and analysis, decision to publish, or preparation of the manuscript.

Conflict of interest

Prof. Josep M. Llovet is receiving research support from Bayer HealthCare Pharmaceuticals, Eisai Inc, Bristol-Myers Squibb and Ipsen, and consulting fees from Bayer HealthCare Pharmaceuticals, Bristol-Myers Squibb, Eisai Inc, Celsion Corporation, Eli Lilly, Exelixis, Merck, Ipsen, Glycotest, Navigant, Leerink Swann LLC, Midatech Ltd, Fortress Biotech, Sprink Pharmaceuticals and Nucleix and CANFITE. CA has a research contract with CHIOME Biosciences Inc. The other authors report no conflicts of interest in this work.

Please refer to the accompanying ICMJE disclosure forms for further details.

Authors' contributions

JCR designed, performed research, analyzed all data, and wrote the results; LT designed, performed research and reviewed the manuscript; MSC designed and performed research; JAF, LR, MV, NV and SR performed research; LN, MA and MM performed bioinformatics analyses of transcriptomic, genomic and epigenetic data; BL and NA developed and performed RNA variant and editing analysis and BL, DS and NA performed expression analyses of RNA-seq data; OK, performed research; AV performed PDX experiment; SC, RK, MAB, BM and PC provided clinical samples, the associated relevant clinical and pathological information and critically review the manuscript; MDS; performed research and critically review the manuscript; AS, CS, LG, MGa, MGo, MEM, SB, GR, MLS, GG, YM, NGA, JJU, BLI, BT, MF, RLA, JAS, CP, VB, GL, CB, CG, FH, RP, HM, AC and MS provided clinical samples as well as the associated relevant clinical and pathological information; JB, DP, LS and MJ designed and performed research; MRS, designed, analyzed data, and reviewed the manuscript; JML designed research and supervised the study. CA designed research, analyzed data, supervised the whole study and wrote the manuscript.

Acknowledgements

We thank patients and their families for allowing the collection of biological samples. We also would like to acknowledge the support of the Spanish Group for the Study Of Childhood Liver Cancer of the Spanish Society of Paediatric Haematology and Oncology (SEHOP) and the clinical staff of Spanish hospitals that provided us with samples and clinical data (Maciej Murawski, Marta Villa, Sandra Pisa, Montserrat Torrent, Pablo Trujillo, Ester

at 26 days of treatment. Other statistical analysis performed were ANOVA test with the Tukey post-test[†] and unpaired *t* test[‡] (**p* < 0.05; ***p* ≤ 0.001; ****p* < 0.0001). CHKA, choline kinase alpha; HTA, Human Transcriptome Array; MRS, Molecular Risk Stratification; PDX, patient-derived xenograft; RNA-seq, RNA sequencing; RT-qPCR, reverse transcription quantitative PCR; siRNA, small interfering RNA.

Anton, Jose Andres Molino, Hermenegildo González, M^a Esther Llinares, José Luis Fuster and Isabel Ojanguren). We thank the IGTP Biobank and Genomic Units and the HUVR-IBiS Biobank (Andalusian Public Health System Biobank and ISCIII-Red de Biobancos PT17/0015/0041) for the assessment and technical support provided. We also thank Dr. Eduard Cabré for his advice on statistical analysis. We acknowledge the personnel at the Genome Analysis Platform of CIC bioGUNE and CIBERehd for their help on experimental design and for processing the methylation Beadchips. We acknowledge Koji Nakamura (CHIOME Biosciences Inc) for kindly providing DLK1 antibody. We thank Ugne Balaseviciute for her assistance in experimental procedures.

Supplementary data

Supplementary data to this article can be found online at <https://doi.org/10.1016/j.jhep.2020.03.025>.

References

Author names in bold designate shared co-first authorship

- [1] Schnater JM, Köhler SE, Lamers WH, Von Schweinitz D, Aronson DC. Where do we stand with hepatoblastoma? A review. *Cancer* 2003;98:668–678.
- [2] Linabery AM, Ross JA. Trends in childhood cancer incidence in the U.S. (1992–2004). *Cancer* 2008;112:416–432.
- [3] Kehm RD, Spector LG, Osypuk TL, Poynter JN, Vock DM. Do pregnancy characteristics contribute to rising childhood cancer incidence rates in the United States? *Pediatr Blood Cancer* 2018;65:1–9.
- [4] Aronson DC, Czauderna P, Maibach R, Perilongo G, Morland B. The treatment of hepatoblastoma: its evolution and the current status as per the SIOPEL trials. *J Indian Assoc Pediatr Surg* 2014;19:201–207.
- [5] Semeraro M, Branchereau S, Maibach R, Zsiros J, Casanova M, Brock P, et al. Relapses in hepatoblastoma patients: clinical characteristics and outcome-Experience of the International Childhood Liver Tumour Strategy Group (SIOPEL). *Eur J Cancer* 2013;49:915–922.
- [6] **Meyers RL, Maibach R, Hiyama E, Häberle B, Krailo M, Rangaswami A**, et al. Risk-stratified staging in paediatric hepatoblastoma: a unified analysis from the Children's Hepatic tumors International Collaboration. *Lancet Oncol* 2017;18:122–131.
- [7] Armengol C, Cairo S, Fabre M, Buendia MA. Wnt signaling and hepatocarcinogenesis: the hepatoblastoma model. *Int J Biochem Cell Biol* 2011;43:265–270.
- [8] Perugorria MJ, Olaizola P, Labiano I, Esparza-baquer A, Marzioni M, Marin JJG, et al. Wnt – β -catenin signalling in liver development, health and disease. *Nat Rev Gastroenterol Hepatol* 2019;16:121–136.
- [9] **Cairo S, Armengol C**, De Reyniès A, Wei Y, Thomas E, Renard CA, et al. Hepatic stem-like phenotype and interplay of wnt/ β -catenin and Myc signaling in aggressive childhood liver cancer. *Cancer Cell* 2008;14:471–484.
- [10] Hooks KB, Audoux J, Fazli H, Lesjean S, Ernault T, Senant N-D, et al. New insights into diagnosis and therapeutic options for proliferative hepatoblastoma. *Hepatology* 2018;68:89–102.
- [11] Sumazin P, Chen Y, Treviño LR, Sarabia SF, Hampton OA, Patel K, et al. Genomic analysis of hepatoblastoma identifies distinct molecular and prognostic subgroups. *Hepatology* 2017;65:104–121.
- [12] **Gröbner SN, Worst BC**, Weischenfeldt J, Buchhalter I, Kleinheinz K, Rudneva VA, et al. The landscape of genomic alterations across childhood cancers. *Nature* 2018;555:321–327.
- [13] **Eichenmüller M, Trippel F**, Kreuder M, Beck A, Schwarzmayr T, Häberle B, et al. The genomic landscape of hepatoblastoma and their progenies with HCC-like features. *J Hepatol* 2014;61:1312–1320.
- [14] Buendia MA. Unravelling the genetics of hepatoblastoma: few mutations, what else? *J Hepatol* 2014;61:1202–1204.
- [15] **Maschietto M, Rodrigues TC**, Kashiwabara AY, de Araujo ÉSS, Aguiar TFM, da Costa CML, et al. DNA methylation landscape of hepatoblastomas reveals arrest at early stages of liver differentiation and cancer-related alterations. *Oncotarget* 2017;8:97871–97889.
- [16] **Cui X, Liu B**, Zheng S, Dong K, Dong R. Genome-wide analysis of DNA methylation in hepatoblastoma tissues. *Oncol Lett* 2016;12:1529–1534.
- [17] Honda S, Minato M, Suzuki H, Fujiyoshi M, Miyagi H, Haruta M, et al. Clinical prognostic value of DNA methylation in hepatoblastoma: four novel tumor suppressor candidates. *Cancer Sci* 2016;107:812–819.
- [18] Edgar R, Domrachev M, Lash AE. Gene Expression Omnibus: NCBI gene expression and hybridization array data repository. *Nucleic Acids Res* 2002;30:207–210.
- [19] Tomlinson GE, Douglass EC, Pollock BH, Finegold MJ, Schneider NR. Cytogenetic evaluation of a large series of hepatoblastomas: numerical abnormalities with recurring aberrations involving 1q12-q21. *Genes Chromosomes Cancer* 2005;44:177–184.
- [20] Albrecht S, von Schweinitz D, Waha A, Kraus JA, von Detailing A, Pietsch T. Loss of maternal Alleles on chromosome arm 11p in hepatoblastoma. *Cancer Res* 1994;54:5041–5044.
- [21] López-Terrada D, Alaggio R, de Dávila MT, Czauderna P, Hiyama E, Katzenstein H, et al. Towards an international pediatric liver tumor consensus classification: proceedings of the Los Angeles COG liver tumors symposium. *Mod Pathol* 2014;27:472–491.
- [22] Levanon EY, Hallegger M, Kinar Y, Shemesh R, Djinovic-Carugo K, Rechavi G, et al. Evolutionarily conserved human targets of adenosine to inosine RNA editing. *Nucleic Acids Res* 2005;33:1162–1168.
- [23] Nishikura K. Functions and regulation of RNA editing by ADAR deaminases. *Annu Rev Biochem* 2010;79:321–349.
- [24] da Rocha ST, Edwards CA, Ito M, Ogata T, Ferguson-Smith AC. Genomic imprinting at the mammalian Dlk1-Dio3 domain. *Trends Genet* 2008;24:306–316.
- [25] Benetatos L, Hatzimichael E, London E, Vartholomatos G. The microRNAs within the Dlk1-DIO3 genomic region: involvement in disease pathogenesis. *Cell Mol Life Sci* 2013;70:795–814.
- [26] **López-Terrada D, Gunaratne PH**, Adesina AM, Pulliam J, Hoang DM, Nguyen Y, et al. Histologic subtypes of hepatoblastoma are characterized by differential canonical Wnt and Notch pathway activation in Dlk1+ precursors. *Hum Pathol* 2009;40:783–794.
- [27] **Van de Wetering M, Sancho E**, Verweij C, De Lau W, Oving I, Hurlstone A, et al. The β -catenin/TCF-4 complex imposes a crypt progenitor phenotype on colorectal cancer cells. *Cell* 2002;111:241–250.
- [28] Zimmermann A. The emerging family of hepatoblastoma tumours: from ontogenesis to oncogenesis. *Eur J Cancer* 2005;41:1503–1514.
- [29] **Donsante A, Miller DG**, Li Y, Vogler C, Brunt EM, Russell DW, et al. AAV vector integration sites in Mouse hepatocellular carcinoma. *Science* 2007;317:477.
- [30] **Wang P-R, Xu M**, Toffanin S, Li Y, Llovet JM, Russell DW. Induction of hepatocellular carcinoma by in vivo gene targeting. *Proc Natl Acad Sci U S A* 2012;109:11264–11269.
- [31] Harada K, Toyooka S, Maitra A, Maruyama R, Toyooka KO, Timmons CF, et al. Aberrant promoter methylation and silencing of the RASSF1A gene in pediatric tumors and cell lines. *Oncogene* 2002;21:4345–4349.
- [32] **Chow RKK, Sin ST-K**, Liu M, Li Y, Chan THM, Song Y, et al. AKR7A3 suppresses tumorigenicity and chemoresistance in hepatocellular carcinoma through attenuation of ERK, c-Jun and NF- κ B signaling pathways. *Oncotarget* 2017;8:83469–83479.
- [33] Chen C, Wang L, Liao Q, Huang Y, Ye H, Chen F, et al. Hypermethylation of EDNRB promoter contributes to the risk of colorectal cancer. *Diagn Pathol* 2013;8:909.
- [34] Deloria AJ, Höflmayer D, Kienzl P, Łopatecka J, Sampl S, Klimpfinger M, et al. Epithelial splicing regulatory protein 1 and 2 paralogs correlate with splice signatures and favorable outcome in human colorectal cancer. *Oncotarget* 2016;7:73800–73816.
- [35] Tessitore L, Sesca E, Vance DE. Inactivation of phosphatidylethanolamine N-methyltransferase-2 in aflatoxin-induced liver cancer and partial reversion of the neoplastic phenotype by PEMT transfection of hepatoma cells. *Int J Cancer* 2000;86:362–367.
- [36] Zhang F, Sun H, Zhang S, Yang X, Zhang G, Su T. Overexpression of PER3 inhibits self-renewal capability and chemoresistance of colorectal cancer stem-like cells via inhibition of notch and β -catenin signaling. *Oncol Res Featur Preclin Clin Cancer Ther* 2017;25:709–719.
- [37] Aoyama C, Liao H, Ishidate K. Structure and function of choline kinase isoforms in mammalian cells. *Prog Lipid Res* 2004;43:266–281.
- [38] de la Cueva A, Ramírez de Molina A, Álvarez-Ayerza N, Ramos MA, Cebrían A, del Pulgar TG, et al. Combined 5-FU and ChoK α inhibitors as a new alternative therapy of colorectal cancer: evidence in

- human tumor-derived cell lines and mouse xenografts. *PLoS One* 2013;8:1–13.
- [39] Paz-Yaacov N, Bazak L, Buchumenski I, Porath HT, Danan-Gotthold M, Knisbacher BA, et al. Elevated RNA editing activity is a major contributor to transcriptomic diversity in tumors. *Cell Rep* 2015;13:267–276.
- [40] Kung C-P, Maggi LB, Weber JD. The role of RNA editing in cancer development and Metabolic Disorders. *Front Endocrinol (Lausanne)* 2018;9:1–21.
- [41] Galeano F, Leroy A, Rossetti C, Gromova I, Gautier P, Keegan LP, et al. Human BLCAP transcript: new editing events in normal and cancerous tissues. *Int J Cancer* 2010;127:127–137.
- [42] Gromova I, Romov P, Celis JE. bc10 : a novel human bladder cancer-associated protein with a conserved genomic structure downregulated in invasive cancer. *Int J Cancer* 2002;546:539–546.
- [43] Han L, Diao L, Yu S, Xu X, Li JBJ, Zhang R, et al. The genomic landscape and clinical relevance of A-to-I RNA editing in human cancers. *Cancer Cell* 2015;28:515–528.
- [44] Hu X, Wan S, Ou Y, Zhou B, Zhu J, Yi X, et al. RNA over-editing of BLCAP contributes to hepatocarcinogenesis identified by whole-genome and transcriptome sequencing. *Cancer Lett* 2015;357:510–519.
- [45] Paz N, Levanon EY, Amariglio N, Heimberger AB, Ram Z, Constantini S, et al. Altered adenosine-to-inosine RNA editing in human cancer. *Genome Res* 2007;17:1586–1595.
- [46] Chen W, He W, Cai H, Hu B, Zheng C, Ke X, et al. A-to-I RNA editing of BLCAP lost the inhibition to STAT3 activation in cervical cancer. *Oncotarget* 2017;8:39417–39429.
- [47] Zhao M, Zhang L, Qiu X, Zeng F, Chen W, An Y, et al. BLCAP arrests G1/S checkpoint and induces apoptosis through downregulation of pRb1 in HeLa cells. *Oncol Rep* 2016;35:3050–3058.
- [48] Luk JM, Burchard J, Zhang C, Liu AM, Wong KF, Shek FH, et al. DLK1-DIO3 genomic imprinted microRNA cluster at 14q32.2 defines a stemlike subtype of hepatocellular carcinoma associated with poor survival. *J Biol Chem* 2011;286:30706–30713.
- [49] Benetatos L, Vartholomatos G, Stem ÁMÁ. DLK1-DIO3 imprinted cluster in induced pluripotency: landscape in the mist. *Cell Mol Life Sci* 2014;71:4421–4430.
- [50] Wang P, Xu M, Toffanin S, Li Y, Llovet JM, Russell DW. Induction of hepatocellular carcinoma by in vivo gene targeting. *Proc Natl Acad Sci U S A* 2012;109:11264–11269.
- [51] Toffanin S, Hoshida Y, Lachenmayer A, Villanueva A, Cabellos L, Mínguez B, et al. MicroRNA-based classification of hepatocellular carcinoma and oncogenic role of miR-517a. *Gastroenterology* 2011;140:1618–1628.
- [52] Pujadas E, Feinberg AP. Regulated noise in the epigenetic landscape of development and disease. *Cell* 2012;148:1123–1131.
- [53] Kulis M, Esteller M. DNA methylation and cancer. *Adv Genet* 2010;70:27–56.
- [54] Ramírez de Molina A, Gutiérrez R, Ramos MA, Silva JM, Silva J, Bonilla F, et al. Increased choline kinase activity in human breast carcinomas: clinical evidence for a potential novel antitumor strategy. *Oncogene* 2002;21:4317–4322.
- [55] Lin X-M, Hu L, Gu J, Wang R-Y, Li L, Tang J, et al. Choline kinase α mediates interactions between the epidermal growth factor receptor and mechanistic target of rapamycin complex 2 in hepatocellular carcinoma cells to promote drug resistance and xenograft tumor progression. *Gastroenterology* 2017;152:1187–1202.
- [56] de Molina AR, Sarmentero-Estrada J, Belda-Iniesta C, Tarón M, de Molina VR, Cejas P, et al. Expression of choline kinase alpha to predict outcome in patients with early-stage non-small-cell lung cancer: a retrospective study. *Lancet Oncol* 2007;8:889–897.
- [57] Asim M, Massie CE, Orafidiya F, Pértiga-Gomes N, Warren AY, Esmaeili M, et al. Choline kinase alpha as an androgen receptor chaperone and prostate cancer therapeutic target. *J Natl Cancer Inst* 2015;108:djv371.
- [58] Hernández-Alcoceba R, Fernández F, Lacal JC. In vivo antitumor activity of choline kinase inhibitors: a novel target for anticancer drug discovery. *Cancer Res* 1999;59:3112–3118.